Supplementary Information (SI) for Journal of Materials Chemistry C.

Design of alkali lead oxybromides with strong second-harmonic generation response and large birefringence

Jialin Zeng[a,b], Shuangcheng Li[a], Yahui Zhu[a], Zilong Geng[a,d], Yiting Luo[a,b], Ruibiao Fu[*a,d] and Zuju Ma[*c]

[a]State Key Laboratory of Structural Chemistry, Fujian Institute of Research on the Structure of Matter, Chinese Academy of Sciences, Fuzhou, Fujian 350002, P. R. China

[b]College of Chemistry and Materials Science, Fujian Normal University, Fuzhou, Fujian 350007, P. R. China

[c]School of Environmental and Materials Engineering, Yantai University, Yantai, 264005, P. R. China

[d]University of Chinese Academy of Sciences, Beijing 100049, China

[*]Corresponding author. *E-mail addresses:* furb@fjirsm.ac.cn (R. B. Fu), zjma@outlook.com (Z. J. Ma).

Computational Details

In the static case, the imaginary part of the static second-order optical susceptibility can be expressed as:

$$\chi^{abc} = \frac{e^3}{\hbar^2\Omega}\sum_{nml,k}\frac{r^{a}_{nm}(r^{b}_{ml}r^{c}_{ln} + r^{c}_{ml}r^{b}_{ln})}{2\omega_{nm}\omega_{ml}\omega_{ln}}[\omega_n f_{ml} + \omega_m f_{ln} + \omega_l f_{nm}]$$

$$+ \frac{ie^3}{4\hbar^2\Omega}\sum_{nm,k}\frac{f_{nm}}{\omega^2_{mn}}[r^{a}_{nm}(r^{b}_{mn;c} + r^{c}_{mn;b}) + r^{b}_{nm}(r^{a}_{mn;c} + r^{c}_{mn;a}) + r^{c}_{nm}(r^{a}_{mn;b} + r^{b}_{mn;a})]$$

where r is the position operator, $\hbar\omega_{nm} = \hbar\omega_n - \hbar\omega_m$ is the energy difference for the bands m and n, $f_{mn} = f_m - f_n$ is the difference of the Fermi distribution functions, subscripts a, b, and c are Cartesian indices, and $r^{b}_{mn;a}$ is the so-called generalized derivative of the coordinate operator in k space.

$$r^{b}_{nm;a} = \frac{r^{a}_{nm}\Delta^{b}_{mn} + r^{b}_{nm}\Delta^{a}_{mn}}{\omega_{nm}} + \frac{i}{\omega_{nm}} \times \sum_{l}(\omega_{lm}r^{a}_{nl}r^{b}_{lm} - \omega_{nl}r^{b}_{nl}r^{a}_{lm})$$

where $\Delta^{a}_{nm} = (p^{a}_{nn} - p^{a}_{mm}) / m$ is the difference between the electronic velocities at the bands n and m.

The $\chi^{(2)}$ coefficients here were calculated from PBE wave functions with a 3×5×5 (for **$Rb_3[Pb_2Br_5(OOC(CH_2)_3COO)]$**)/5×3×5 (for **$Cs_3[Pb_2Br_5(OOC(CH_2)_3COO)]$**) k-point grid and about 512 bands. A scissor operator has been added to correct the conduction band energy (corrected to the experimental gap), which has been proved to be reliable in predicting the second-order susceptibility for semiconductors and insulators.[1-3]

For an external radiation electric field E, the dipole moment μ_i of a group can be

expressed as a Taylor series expansion [4, 5]

$$\mu_i = \mu_i^0 + \alpha_{ij}E_j + \frac{1}{2!}\beta_{ijk}E_jE_k + \frac{1}{3!}\gamma_{ijkl}E_jE_kE_l$$

where *i*, *j*, *k*, and *l* subscripts represent the different Cartesian coordinate components *x*, *y*, or *z*. μ_i^0 is the permanent dipole moment of a group, namely the dipole moment without an applied electric field. Physical quantities α, β and γ correspond to the linear polarizability (α, which corresponds to the linear optical coefficient of a group), first-order hyperpolarizability tensor (β, which is the second-order nonlinear optical coefficient of a group), and second-order hyperpolarizability tensor (γ, which is the third-order nonlinear optical coefficient of a group).

We calculate the static linear polarizability (α) and static first-order hyperpolarizability (β) of [$PbBr_4O_2$] and [$OOC(CH_2)_3COO$] groups at the PBE1PBE level [6] of theory with a reasonably large basis set def2TZVP [7,8] by using the Gaussian 09 program.[9] The polarizability anisotropy ($\Delta\alpha$) was obtained by the following formula to reflect the sources of birefringence.[10]

$$\Delta\alpha = \sqrt{\left[\left(\alpha_{xx} - \alpha_{yy}\right)^2 + \left(\alpha_{xx} - \alpha_{zz}\right)^2 + \left(\alpha_{yy} - \alpha_{zz}\right)^2\right]/2}$$

. Tables and Figures

Table S1. Crystal data and structure refinements for **$Rb_3[Pb_2Br_5(OOC(CH_2)_3COO)]$**.

Empirical formula	**$Rb_3[Pb_2Br_5(OOC(CH_2)_3COO)]$**
Formula weight	1200.44
Temperature(K)	298(2)
Crystal color	Colorless
Wavelength(Å)	1.54184
Crystal system	Orthorthombic
Space group	*Imm2*
a / Å	20.9890(3)
b / Å	11.98510(10)
c / Å	8.00740(10)
α / °	90
β / °	90
γ / °	90
Volume / $Å^3$	2014.30(4)
Z	4
Absorption correction	multi-scan
Crystal size	0.3 mm × 0.1 mm × 0.1 mm
ρ_{calcd} / $g \cdot cm^{-3}$	3.958
μ / mm^{-1}	52.558
F(000)	2072
Data / restraints / parameters	1875/1/100
2-Theta range for data collection	8.429 to 149.944
Limiting indices	$-26 \le h \le 26$, $-14 \le k \le 15$, $-7 \le l \le 7$
Reflections collected / unique	9430/1875 [Rint=0.0453]
Completeness	100%
Goodness-of-fit on F^2	1.072
R_1,wR_2 ($I > 2\sigma$) [a]	$R_1 = 0.0293$, $wR_2 = 0.0818$
R_1,wR_2 (all data)	$R_1 = 0.0297$, $wR_2 = 0.0821$
Largest diff. peak and hole/ $e \cdot Å^{-3}$	1.59 and -1.43
Flack parameter	-0.027(11)

[a] $R_1 = \Sigma||F_o| - |F_c||/\Sigma|F_o|$ and $wR_2 = [\Sigma w(Fo^2 - Fc^2)^2/ \Sigma wF_o^4]^{1/2}$.

Table S2. Crystal data and structure refinements for **$Cs_3[Pb_2Br_5(OOC(CH_2)_3COO)]$**.

Empirical formula	**$Cs_3[Pb_2Br_5(OOC(CH_2)_3COO)]$**
Formula weight	1342.76
Temperature(K)	293(2)
Crystal color	Colorless
Wavelength(Å)	1.54184
Crystal system	Orthorthombic
Space group	*Amm2*
a / Å	12.26789(19)
b / Å	21.5634(4)
c / Å	7.97808(15)
α / °	90
β / °	90
γ / °	90
Volume / $Å^3$	2110.50(6)
Z	4
Absorption correction	multi-scan
Crystal size	0.2 mm × 0.1 mm × 0.1 mm
ρ_{calcd} / $g \cdot cm^{-3}$	4.226
μ / mm^{-1}	81.548
F(000)	2288.0
Data / restraints / parameters	2257/1/101
2-Theta range for data collection	7.206 to 149.536
Limiting indices	-13 ≤h ≤ 15,-20≤K≤26,-9≤1≤9
Reflections collected / unique	10429/2257 [Rint=0.0575]
Completeness	100%
Goodness-of-fit on F^2	1.067
R_1,wR_2 ($I > 2\sigma$) [a]	R_1 = 0.0462, wR_2 = 0.1164
R_1,wR_2 (all data)	R_1 = 0.0468, wR_2 = 0.1175
Largest diff. peak and hole/ $e \cdot Å^{-3}$	1.25 and -1.09
Flack parameter	-0.004(7)

[a] $R_1 = \Sigma||F_o| - |F_c||/\Sigma|F_o|$ and $wR_2 = [\Sigma w(Fo^2 - Fc^2)^2/ \Sigma wF_o^4]^{1/2}$.

Table S3. Atomic coordinates, equivalent isotropic displacement parameters (Å^2) and BVS for **$Rb_3[Pb_2Br_5(OOC(CH_2)_3COO)]$**.

Atom	*Wyck.*	*x*	*Y*	*z*	U_{eq}[a]	BVS[b]
Pb1	8e	0.35893(2)	0.2516(3)	0.31018(16)	0.0241(2)	2.02
Rb1	2a	0.5	0.5	0.396(3)	0.0285(5)	1.13
Rb2	2b	0.5	0	0.5215(4)	0.0359(6)	0.98
Rb3	4c	0.31151(13)	0	0.7167(4)	0.0666(8)	0.79
Rb4	4c	0.31014(10)	0.5	0.7193(3)	0.0485(5)	0.82
Br1	4c	0.35755(9)	0.5	0.1758(4)	0.0414(5)	-0.82
Br2	8e	0.23558(7)	0.26759(14)	0.4736(2)	0.0447(4)	-0.74
Br3	4c	0.34955(11)	0	0.2662(5)	0.0626(10)	-1.03
Br4	4d	0.5	0.21964(18)	0.2375(3)	0.0329(4)	-0.94
O1	8e	0.3993(4)	0.1722(7)	0.5889(14)	0.038(2)	-2.00
O2	8e	0.4047(4)	0.3536(7)	0.5583(11)	0.031(17)	-2.15
C1	8e	0.4131(6)	0.2681(10)	0.642(18)	0.029(3)	
C2	4d	0.5	0.3454(12)	0.837(20)	0.034(4)	
C3	8e	0.4395(6)	0.2777(15)	0.819(30)	0.051(4)	

[a]U_{eq} is defined as 1/3 of the trace of the orthogonalisedU_{ij} tensor.

[b]Bond valence sums were calculated by the equation：$s = \exp[(R_0 - R_i)/b]$, where R_0 and b are the bond valence parameters and R_i is the observed bond lengths.

Table S4. Atomic coordinates, equivalent isotropic displacement parameters (Å^2) and BVS for **$Cs_3[Pb_2Br_5(OOC(CH_2)_3COO)]$**.

Atom	*Wyck.*	*x*	*y*	*z*	U_{eq}[a]	BVS[b]
Pb1	8f	0.24769(3)	0.3596(2)	0.5859(2)	0.0344(7)	1.90
Cs1	4e	0.5	0.30754(8)	0.1727(2)	0.0482(8)	0.98
Cs2	2b	0.5	0.5	0.5141(3)	0.0361(8)	1.47
Cs3	4d	0	0.31582(9)	0.1386(3)	0.0604(9)	0.89
Cs4	2a	0	0.5	0.3718(3)	0.0408(8)	1.22
Br1	4e	0.5	0.35609(13)	0.7121(5)	0.0523(10)	-0.93
Br2	8f	0.25203(12)	0.24121(10)	0.4125(4)	0.048(9)	-0.94
Br3	4d	0	0.3513(14)	0.6474(5)	0.058(11)	-0.95
Br4	4c	0.2193(2)	0.5	0.6636(3)	0.0397(8)	-0.78
O1	8f	0.3515(9)	0.405(6)	0.3402(16)	0.039(2)	-2.13
O2	8f	0.1731(10)	0.3992(6)	0.3092(17)	0.045(3)	-1.89
C1	8f	0.2632(13)	0.4132(7)	0.2580(20)	0.032(3)	
C2	8f	0.2761(18)	0.4405(8)	0.79(30)	0.048(3)	
C3	4c	0.3417(15)	0.5	0.63(30)	0.038(4)	

[a]U_{eq} is defined as 1/3 of the trace of the orthogonalisedU_{ij} tensor.

[b]Bond valence sums were calculated by the equation：$s = \exp[(R_0 - R_i)/b]$, where R_0 and b are the bond valence parameters and R_i is the observed bond lengths.

Table S5. Anisotropic displacement parameters (Å^2) for **$Rb_3[Pb_2Br_5(OOC(CH_2)_3COO)]$**.

Atom	U_{11}	U_{22}	U_{33}	U_{23}	U_{13}	U_{12}
Pb1	0.0184(3)	0.0236(3)	0.0302(3)	0.00211(15)	-0.0027(2)	-0.00039(10)
Rb1	0.0227(8)	0.0251(9)	0.0378(13)	0.0000	0.0000	0.0000
Rb2	0.0285(10)	0.0233(9)	0.0561(17)	0.0000	0.0000	0.0000
Rb3	0.0568(13)	0.0407(11)	0.102(2)	0.0000	0.0433(14)	0.0000
Rb4	0.0331(9)	0.0463(11)	0.0662(15)	0.0000	0.0102(9)	0.0000
Br1	0.0433(10)	0.0274(8)	0.0535(13)	0.0000	-0.0176(8)	0.0000
Br2	0.0299(7)	0.0659(9)	0.0382(9)	0.0052(8)	0.0091(6)	-0.0014(6)
Br3	0.0426(9)	0.0230(8)	0.122(3)	0.0000	-0.0266(13)	0.0000
Br4	0.0217(7)	0.0449(9)	0.0322(9)	0.0037(9)	0.0000	0.0000
O1	0.031(4)	0.032(4)	0.052(6)	0.008(4)	0.007(4)	0.001(3)
O2	0.028(4)	0.034(4)	0.031(4)	0.003(4)	-0.002(3)	0.002(3)
C1	0.018(5)	0.038(6)	0.031(7)	0.007(5)	0.004(5)	0.000(4)
C2	0.043(8)	0.024(6)	0.034(10)	-0.006(7)	0.0000	0.0000
C3	0.022(5)	0.101(11)	0.030(7)	0.030(11)	0.000(6)	-0.006(6)

Table S6. Anisotropic displacement parameters (Å^2) for **$Cs_3[Pb_2Br_5(OOC(CH_2)_3COO)]$**.

Atom	U_{11}	U_{22}	U_{33}	U_{23}	U_{13}	U_{12}
Pb1	0.0309(8)	0.0304(8)	0.042(8)	0.0001(3)	0.00097(18)	0.00093(13)
Cs1	0.0412(10)	0.0411(10)	0.0623(12)	-0.0056(6)	0.0000	0.0000
Cs2	0.0294(9)	0.0305(10)	0.0486(12)	0.0000	0.0000	0.0000
Cs3	0.0418(10)	0.054(11)	0.0852(17)	-0.0247(9)	0.0000	0.0000
Cs4	0.0268(9)	0.0355(11)	0.0599(13)	0.0000	0.0000	0.0000
Br1	0.0419(14)	0.044(14)	0.071(2)	0.0186(11)	0.0000	0.0000
Br2	0.0517(14)	0.04(12)	0.0523(13)	-0.0091(9)	0.0029(6)	-0.0007(5)
Br3	0.0304(12)	0.0515(15)	0.092(3)	0.0167(14)	0.0000	0.0000
Br4	0.0382(12)	0.0355(12)	0.0455(13)	0.0000	-0.0023(10)	0.0000
O1	0.031(4)	0.044(5)	0.043(5)	0.001(4)	-0.001(4)	0.001(4)
O2	0.039(5)	0.044(5)	0.052(6)	-0.003(5)	-0.008(5)	0.0000
C1	0.043(7)	0.017(6)	0.035(8)	-0.002(5)	-0.013(5)	0.001(4)
C2	0.075(9)	0.041(8)	0.029(7)	0.001(7)	-0.013(10)	-0.008(8)
C3	0.032(8)	0.051(10)	0.032(9)	0.0000	0.007(7)	0.0000

Table S7. Selected bond lengths (**Å**) and angles (deg.) for **$Rb_3[Pb_2Br_5(OOC(CH_2)_3COO)]$**.

Pb(1)-O(1)	2.570(11)	Pb(1)-Br(2)	2.9074(16)
Pb(1)-O(2)	2.523(9)	Pb(1)-Br(3)	3.0423(6)
Pb(1)-Br(1)	3.1657(11)	Pb(1)-Br(4)	3.0417(7)
Rb(1)-Br(1)	3.471(2)	Rb(3)-Br(1)$^{\#6}$	3.564(3)
Rb(1)-Br(1)$^{\#1}$	3.471(2)	Rb(3)-Br(2)	4.076(3)
Rb(1)-Br(4)	3.592(2)	Rb(3)-Br(2)$^{\#5}$	4.076(3)
Rb(1)-Br(4)$^{\#1}$	3.592(2)	Rb(3)-Br(2)$^{\#6}$	3.601(3)
Rb(1)-O(2)	2.961(8)	Rb(3)-Br(2)$^{\#7}$	3.601(3)
Rb(1)-O(2)$^{\#1}$	2.961(8)	Rb(3)-Br(3)	3.695(5)
Rb(1)-O(2)$^{\#2}$	2.961(8)	Rb(3)-O(1)	2.950(9)
Rb(1)-O(2)$^{\#3}$	2.961(8)	Rb(3)-O(1)$^{\#5}$	2.950(9)
Rb(2)-Br(3)	3.762(3)	Rb(4)-Br(1)$^{\#8}$	3.789(4)
Rb(2)-Br(3)$^{\#4}$	3.762(3)	Rb(4)-Br(2)	3.752(2)
Rb(2)-Br(4)	3.479(3)	Rb(4)-Br(2)$^{\#2}$	3.752(2)
Rb(2)-Br(4)$^{\#4}$	3.478(3)	Rb(4)-Br(2)$^{\#7}$	3.919(2)
Rb(2)-O(1)	3.003(9)	Rb(4)-Br(2)$^{\#9}$	3.919(2)
Rb(2)-O(1)$^{\#3}$	3.003(9)	Rb(4)-Br(3)$^{\#7}$	3.373(3)
Rb(2)-O(1)$^{\#4}$	3.003(9)	Rb(4)-O(2)	2.946(8)
Rb(2)-O(1)$^{\#5}$	3.003(9)	Rb(4)-O(2)$^{\#2}$	2.946(8)
C(1)- O(1)	1.260(15)	C(1)- O(2)	1.237(15)
O(1)-Pb(1)-Br(2)	85.8(2)	Br(1)-Pb(1)-Br(3)	153.15(10)
O(1)-Pb(1)-Br(3)	75.8(2)	Br(1)-Pb(1)-Br(4)	93.57(6)
O(1)-Pb(1)-Br(4)	78.4(2)	Br(2)-Pb(1)-Br(3)	93.43(7)
O(2)-Pb(1)-Br(1)	79.36(19)	Br(2)-Pb(1)-Br(4)	163.99(7)
O(2)-Pb(1)-Br(2)	87.28(19)	Br(3)-Pb(1)-Br(4)	85.18(6)
O(2)-Pb(1)-Br(3)	126.6(2)		

Symmetry transformations used to generate equivalent atoms: #1 1 - x,1 - y, z; #2 x, 1 - y, z; #3 1 - x, y, z; #4 1 - x, - y, z; #5 x, - y, z; #6 1/2 - x,- 1/2 + y, 1/2 + z; #7 1/2 - x, 1/2 - y, 1/2 + z; #8 x, y, 1 + z; #9 1/2 - x, 1/2 + y, 1/2 + z.

Table S8. Selected bond lengths (**Å**) and angles (deg.) for **$Cs_3[Pb_2Br_5(OOC(CH_2)_3COO)]$**.

Pb(1)-O(1)	2.534(12)	Pb(1)-Br(2)	2.904(2)
Pb(1)-O(2)	2.537(13)	Pb(1)-Br(3)	3.0831(9)
Pb(1)-Br(1)	3.2558(13)	Pb(1)-Br(4)	3.1098(9)
Cs(1)-Br(1)$^{\#4}$	3.542(3)	Cs(3)-Br(2)	4.114(3)
Cs(1)-Br(1)$^{\#5}$	3.821(4)	Cs(3)-Br(2)$^{\#6}$	3.785(2)
Cs(1)-Br(2)	3.868(2)	Cs(3)-Br(2)$^{\#8}$	4.114(3)
Cs(1)-Br(2)$^{\#3}$	3.868(2)	Cs(3)-Br(2)$^{\#7}$	3.785(2)
Cs(1)-Br(2)$^{\#4}$	3.830(2)	Cs(3)-Br(3)	4.131(5)
Cs(1)-Br(2)$^{\#6}$	3.830(2)	Cs(3)-Br(3)$^{\#5}$	3.993(5)
Cs(1)-O(1)	3.086(12)	Cs(3)-Br(3)$^{\#7}$	3.604(4)
Cs(1)-O(1)$^{\#3}$	3.086(12)	Cs(3)-O(2)	3.098(12)
Cs(2)-Br(1)	3.482(3)	Cs(3)-O(2)$^{\#8}$	3.098(12)
Cs(2)-Br(1)$^{\#2}$	3.482(3)	Cs(4)-Br(3)	3.888(3)
Cs(2)-Br(4)	3.644(3)	Cs(4)-Br(3)$^{\#9}$	3.888(3)
Cs(2)-Br(4)$^{\#2}$	3.644(3)	Cs(4)-Br(4)	3.558(3)
Cs(2)-O(1)	3.072(12)	Cs(4)-Br(4)$^{\#9}$	3.558(3)
Cs(2)-O(1)$^{\#1}$	3.072(12)	Cs(4)-O(2)	3.080(12)
Cs(2)-O(1)$^{\#2}$	3.072(12)	Cs(4)-O(2)$^{\#1}$	3.080(12)
Cs(2)-O(1)$^{\#3}$	3.072(12)	Cs(4)-O(2)$^{\#8}$	3.080(12)
C(1)- O(1)	1.277(19)	Cs(4)-O(2)$^{\#9}$	3.080(12)
C(1)- O(2)	1.22(2)		
O(1)-Pb(1)-O(2)	51.6(4)	O(2)-Pb(1)-Br(4)	78.8(3)
O(1)-Pb(1)-Br(1)	76.7(3)	Br(1)-Pb(1)-Br(2)	96.29(7)
O(1)-Pb(1)-Br(2)	87.8(3)	Br(1)-Pb(1)-Br(3)	153.43(11)
O(1)-Pb(1)-Br(3)	129.8(3)	Br(1)-Pb(1)-Br(4)	93.86(7)
O(1)-Pb(1)-Br(4)	80.5(3)	Br(2)-Pb(1)-Br(3)	92.45(8)
O(2)-Pb(1)-Br(1)	128.3(3)	Br(2)-Pb(1)-Br(4)	162.32(9)
O(2)-Pb(1)-Br(2)	83.6(3)	Br(3)-Pb(1)-Br(4)	85.10(8)
O(2)-Pb(1)-Br(3)	78.6(3)		

Symmetry transformations used to generate equivalent atoms: #1 x,1 - y, z; #2 1 - x, 1 - y, z; #3 1 - x, y, z; #4 1 - x, 1/2 - y, - 1/2 + z; #5 x, y, z - 1; #6 x, 1/2 - y, - 1/2 + z; #7 - x, 1/2 - y, - 1/2 + z; #8 - x, y, z; #9 - x, 1 - y, z.

Table S9. The local dipole moment (μ) in Debye, as well as polarizability anisotropy ($\Delta\alpha$) for eight [$PbBr_4O_2$] polyhedrons and four [$OOC(CH_2)_3COO$] groups in per unit cell of **$Rb_3[Pb_2Br_5(OOC(CH_2)_3COO)]$**. The charge of the structural group was estimated by the Bader charge of each atom.

Dipole moment	μ_x	μ_y	μ_z	μ	$\Delta\boldsymbol{\alpha}$
[$PbBr_4O_2$]	-4.01	0.79	-6.42	7.61	7.22
[$PbBr_4O_2$]	4.01	0.79	-6.42	7.61	7.22
[$PbBr_4O_2$]	-4.01	-0.79	-6.42	7.61	7.22
[$PbBr_4O_2$]	4.01	-0.79	-6.42	7.61	7.22
[$PbBr_4O_2$]	-4.01	0.79	-6.42	7.61	7.22
[$PbBr_4O_2$]	4.01	0.79	-6.42	7.61	7.22
[$PbBr_4O_2$]	-4.01	-0.79	-6.42	7.61	7.22
[$PbBr_4O_2$]	4.01	-0.79	-6.42	7.61	7.22
Sum([$PbBr_4O_2$])	0.00	0.00	-51.36		
[$OOC(CH_2)_3COO$]	0.00	-1.74	7.56	7.76	0.92
[$OOC(CH_2)_3COO$]	0.00	1.74	7.56	7.76	0.92
[$OOC(CH_2)_3COO$]	0.00	-1.74	7.56	7.76	0.92
[$OOC(CH_2)_3COO$]	0.00	1.74	7.56	7.76	0.92
Sum([$OOC(CH_2)_3COO$])	0.00	0.00	30.24		
Total	0.00	0.00	-21.12		

Table S10. The local dipole moment (μ) in Debye, as well as polarizability anisotropy ($\Delta\alpha$) for eight [$PbBr_4O_2$] polyhedrons and four [$OOC(CH_2)_3COO$] groups in per unit cell of **$Cs_3[Pb_2Br_5(OOC(CH_2)_3COO)]$**. The charge of the structural group was estimated by the Bader charge of each atom.

Dipole moment	μ_x	μ_y	μ_z	μ	$\Delta\alpha$
[$PbBr_4O_2$]	1.11	4.35	6.01	7.50	7.02
[$PbBr_4O_2$]	-1.11	4.35	6.01	7.50	7.02
[$PbBr_4O_2$]	-1.11	-4.35	6.01	7.50	7.02
[$PbBr_4O_2$]	1.11	-4.35	6.01	7.50	7.02
[$PbBr_4O_2$]	1.11	4.35	6.01	7.50	7.02
[$PbBr_4O_2$]	-1.11	4.35	6.01	7.50	7.02
[$PbBr_4O_2$]	-1.11	-4.35	6.01	7.50	7.02
[$PbBr_4O_2$]	1.11	-4.35	6.01	7.50	7.02
Sum([$PbBr_4O_2$])	0.00	0.00	48.08		
[$OOC(CH_2)_3COO$]	0.78	0.00	-7.40	7.44	0.76
[$OOC(CH_2)_3COO$]	-0.78	0.00	-7.40	7.44	0.76
[$OOC(CH_2)_3COO$]	0.78	0.00	-7.40	7.44	0.76
[$OOC(CH_2)_3COO$]	-0.78	0.00	-7.40	7.44	0.76
Sum([$OOC(CH_2)_3COO$])	0.00	0.00	-29.6		
Total	0.00	0.00	18.48		

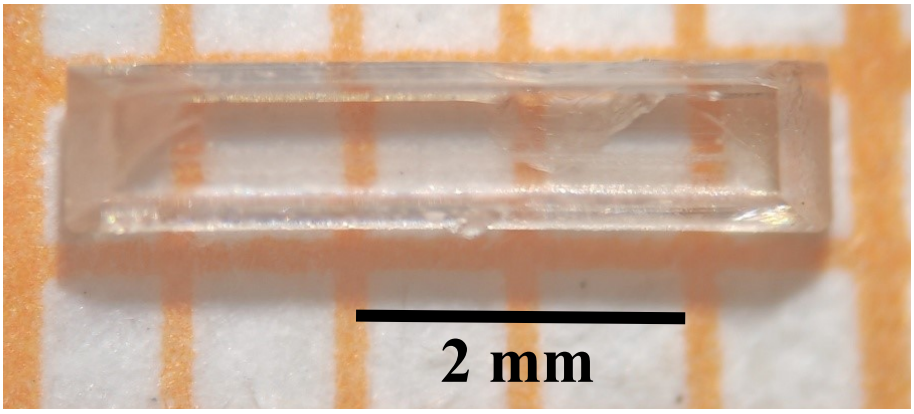

Figure S1. A photograph of the as-grown crystal without polishing for **$Rb_3[Pb_2Br_5(OOC(CH_2)_3COO)]$**.

\

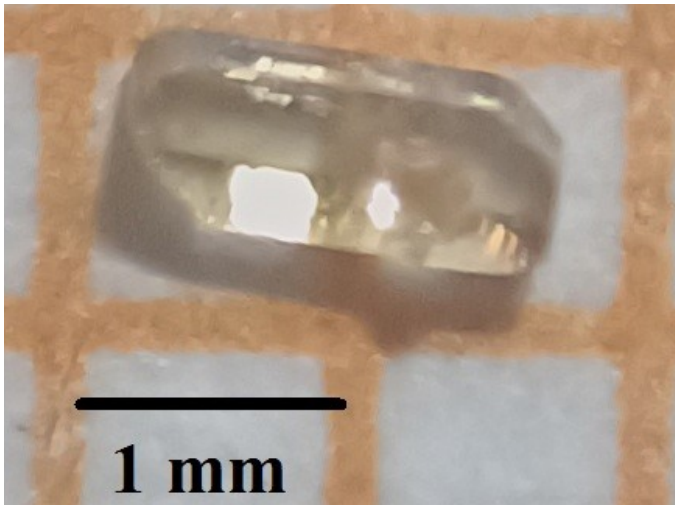

Figure S2. A photograph of the as-grown crystal without polishing for **$Cs_3[Pb_2Br_5(OOC(CH_2)_3COO)]$**.

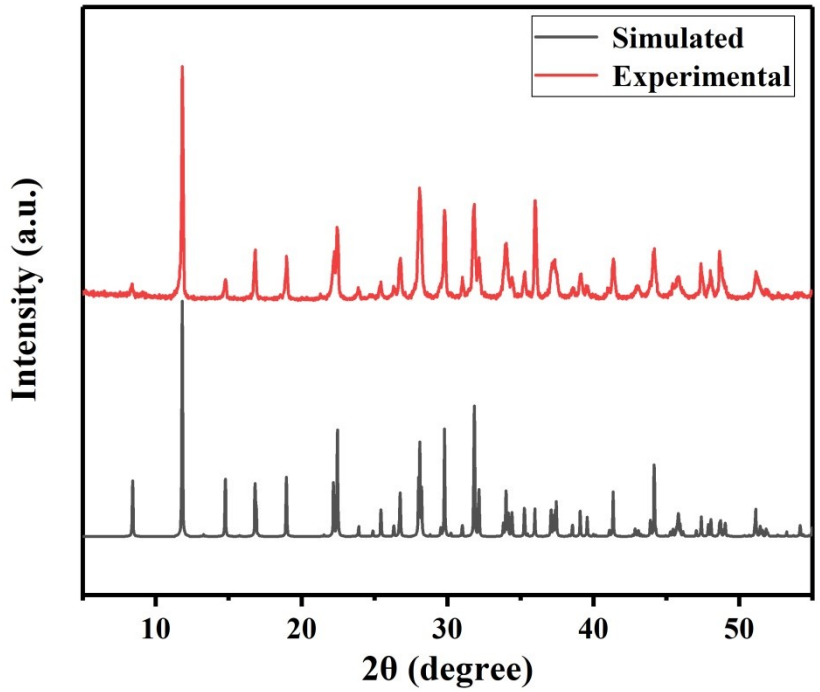

Figure S3. Experimental and simulated PXRD patterns of **$Rb_3[Pb_2Br_5(OOC(CH_2)_3COO)]$**.

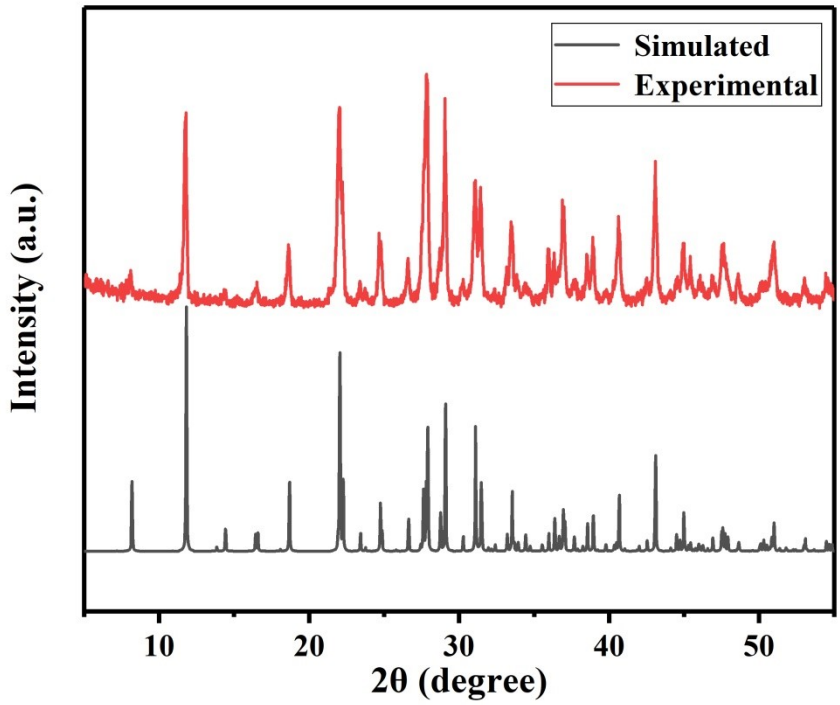

Figure S4. Experimental and simulated PXRD patterns of **$Cs_3[Pb_2Br_5(OOC(CH_2)_3COO)]$**.

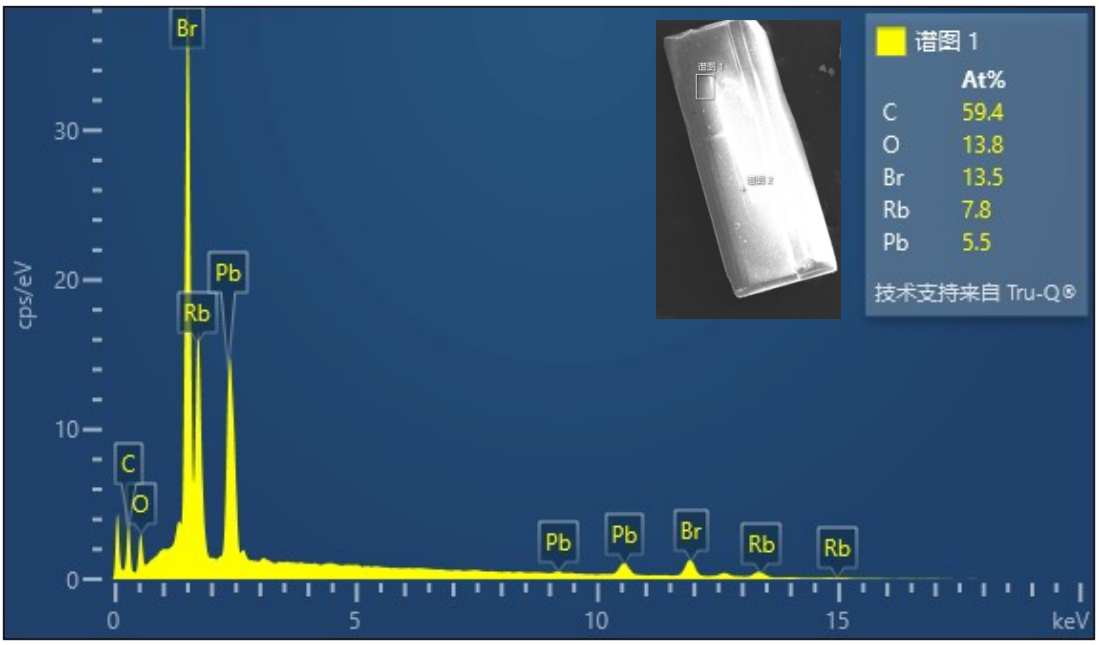

Figure S5. The EDS spectrum of **$Rb_3[Pb_2Br_5(OOC(CH_2)_3COO)]$**.

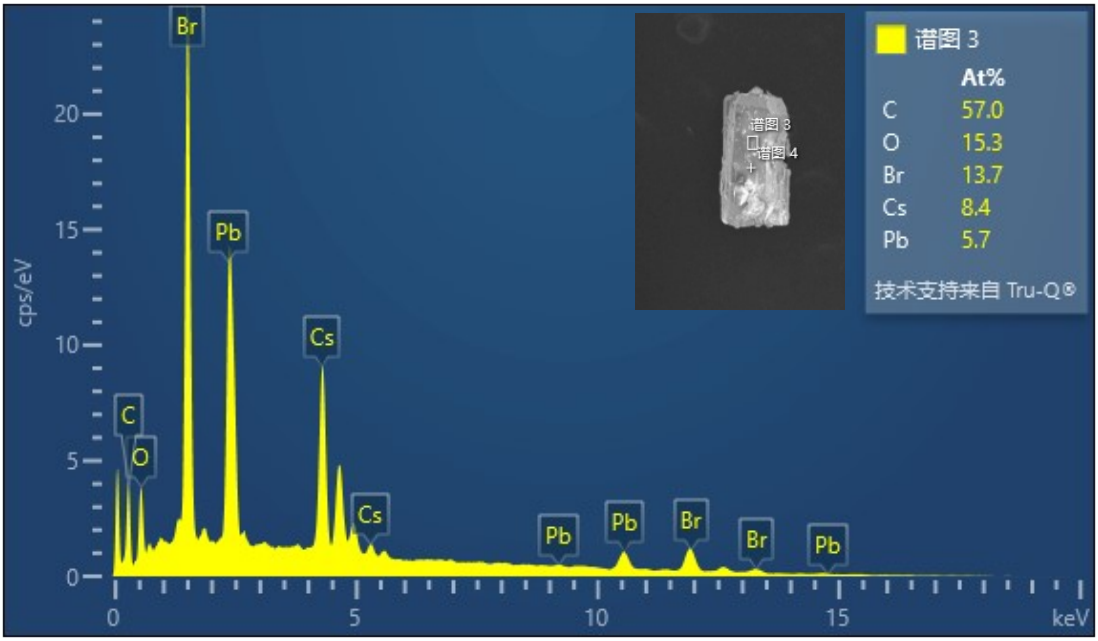

Figure S6. The EDS spectrum of **$Cs_3[Pb_2Br_5(OOC(CH_2)_3COO)]$**.

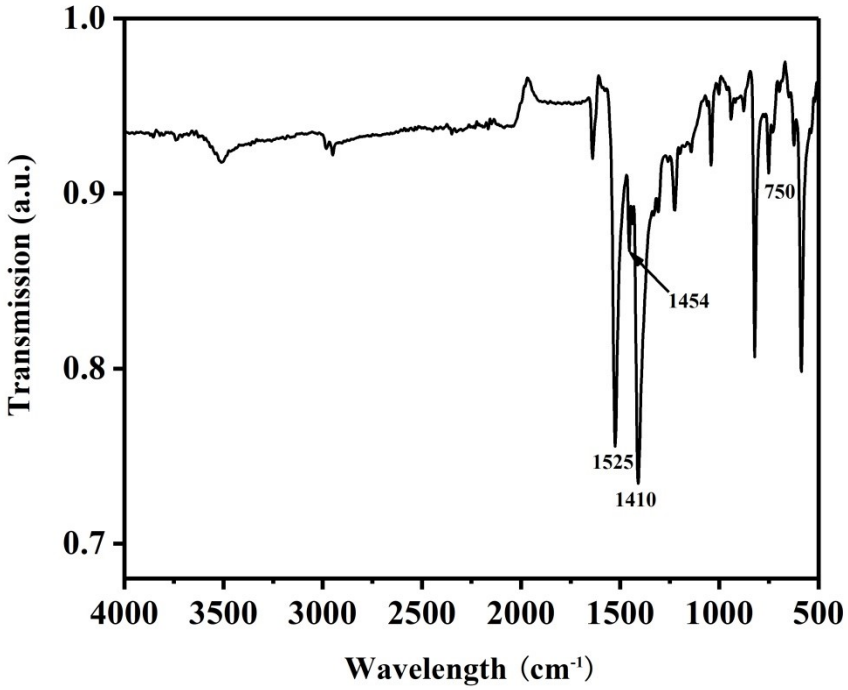

Figure S7. The IR spectrum of **$Rb_3[Pb_2Br_5(OOC(CH_2)_3COO)]$**.

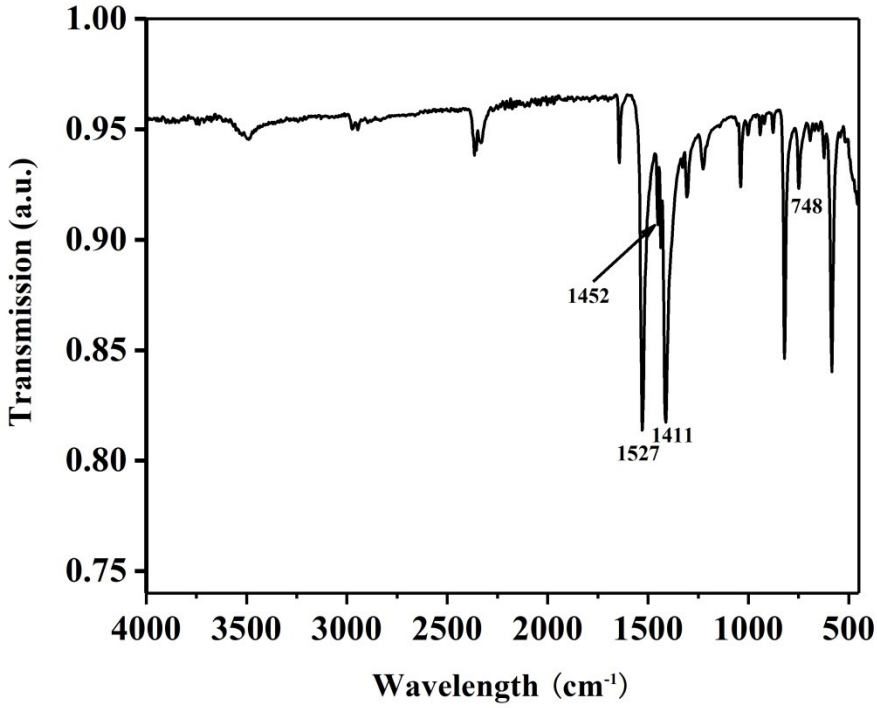

Figure S8. The IR spectrum of **$Cs_3[Pb_2Br_5(OOC(CH_2)_3COO)]$**.

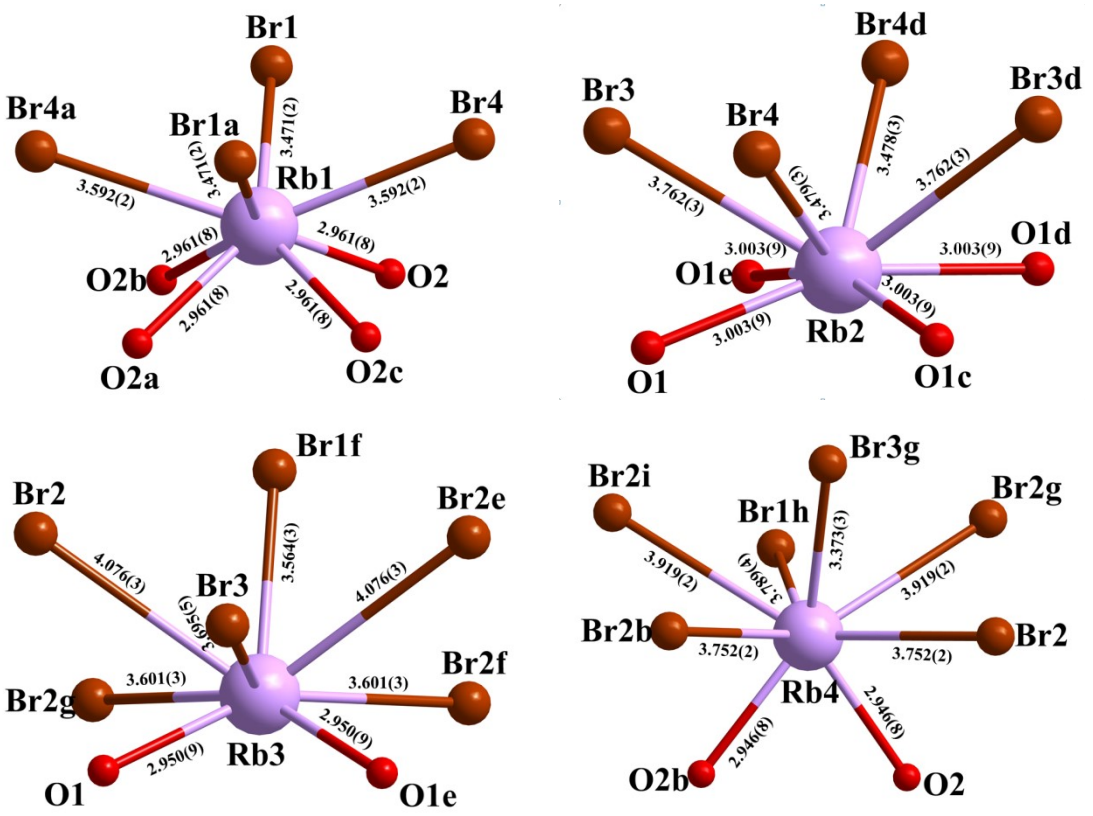

Figure S9. The environments of Rb^+ cations. Symmetry codes: a 1 - x,1 - y, z; b x, 1 - y, z; c 1 - x, y, z; d 1 - x, - y, z; e x, - y, z; f 1/2 - x,- 1/2 + y, 1/2 + z; g 1/2 - x, 1/2 - y, 1/2 + z; h x, y, 1 + z; i 1/2 - x, 1/2 + y, 1/2 + z.

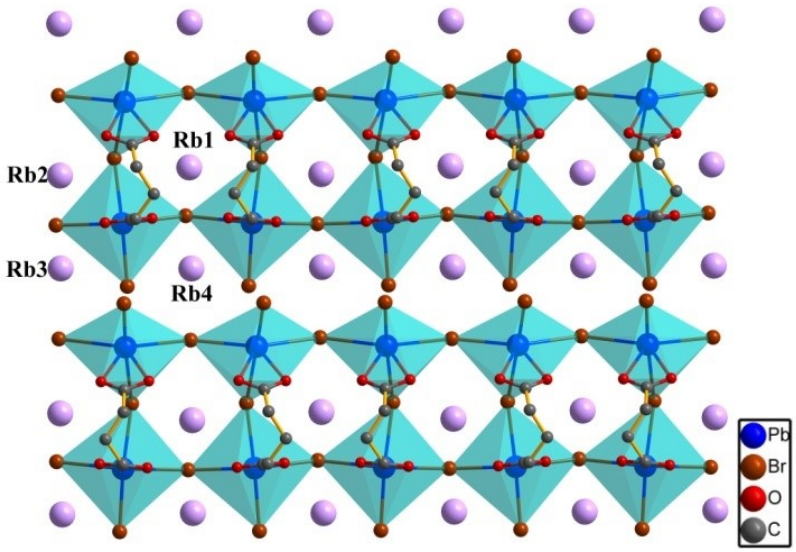

Figure S10. Rb^+ cations are embedded into the double $[Pb_2Br_5(OOC(CH_2)_3COO)]$ chains. Blue-green polyhedron: $[PbBr_4O_2]$.

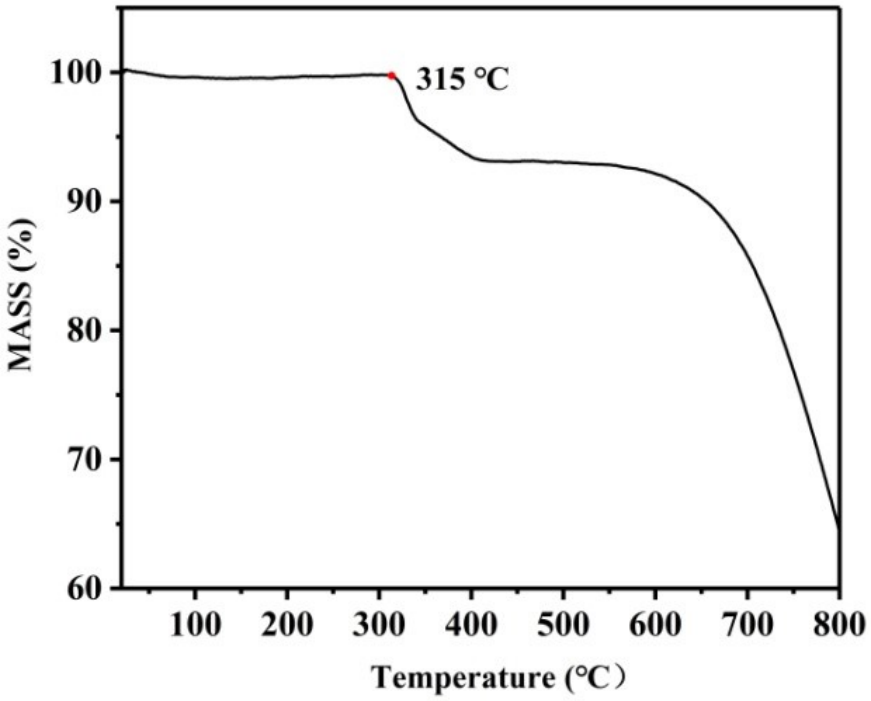

Figure S11. The TGA curve of **$Rb_3[Pb_2Br_5(OOC(CH_2)_3COO)]$**.

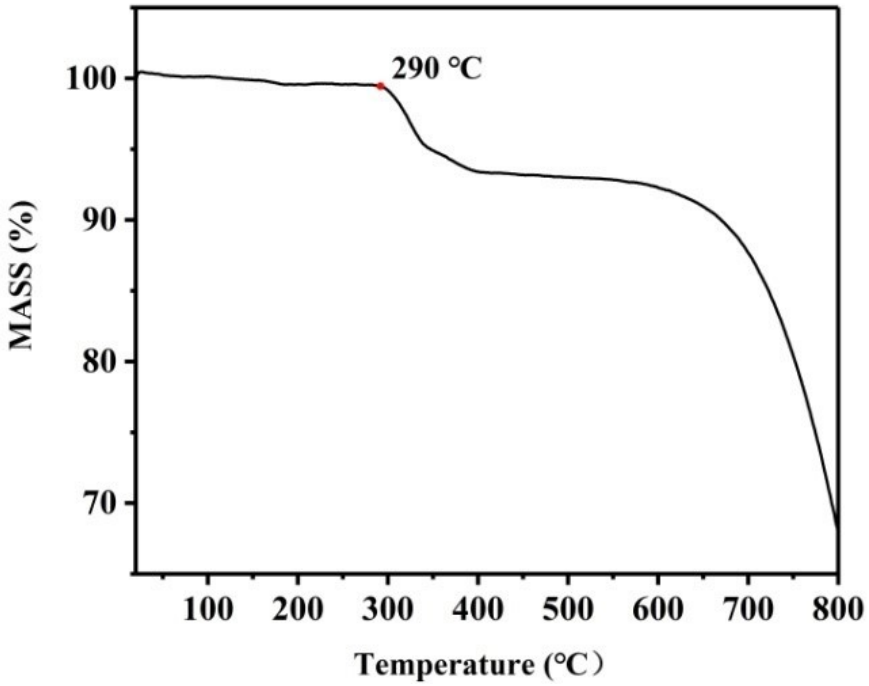

Figure S12. The TGA curve of **$Cs_3[Pb_2Br_5(OOC(CH_2)_3COO)]$**.

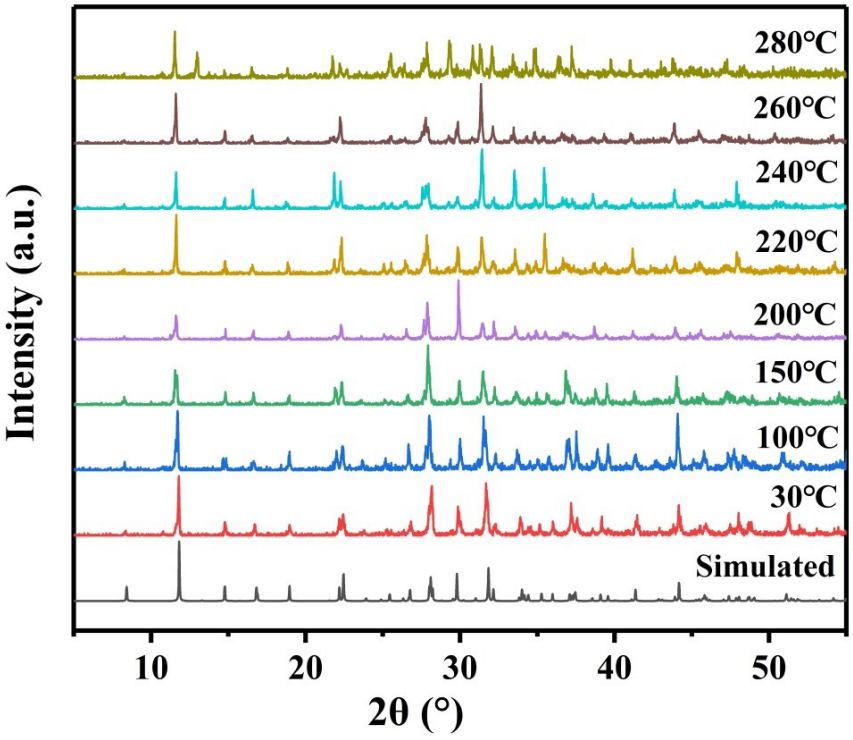

Figure S13. Variable-temperature PXRD patterns of **$Rb_3[Pb_2Br_5(OOC(CH_2)_3COO)]$**.

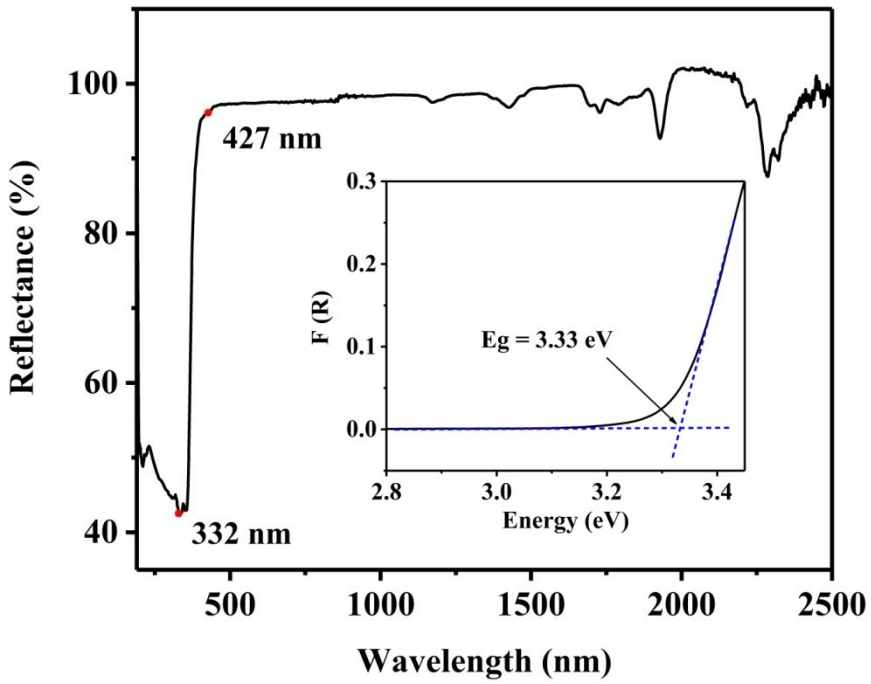

Figure S14. The UV-Vis–NIR spectrum of **$Rb_3[Pb_2Br_5(OOC(CH_2)_3COO)]$**. Inset: the optical band gap.

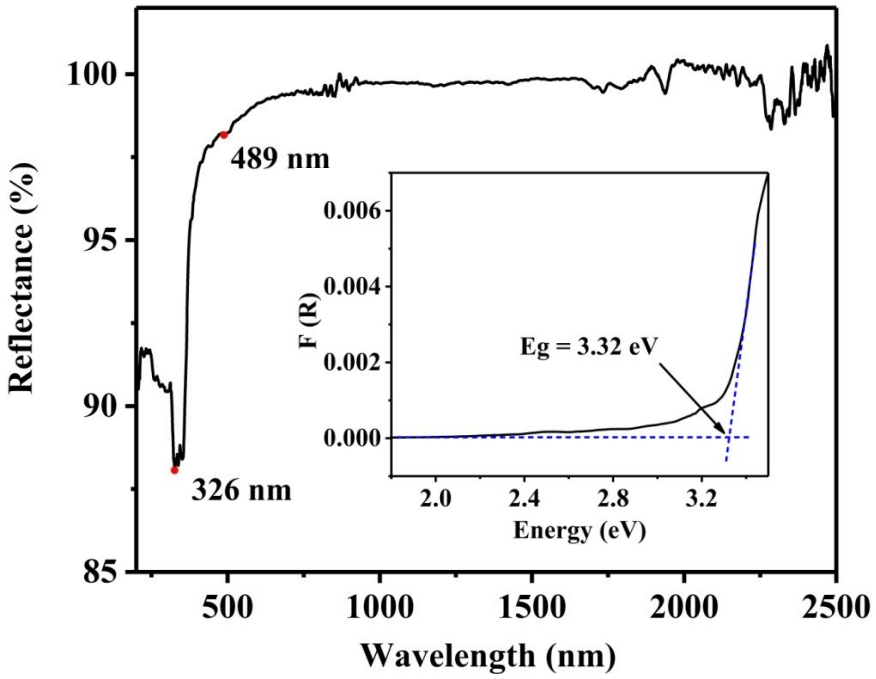

Figure S15. The UV-Vis–NIR spectrum of **$Cs_3[Pb_2Br_5(OOC(CH_2)_3COO)]$**. Inset: the optical band gap.

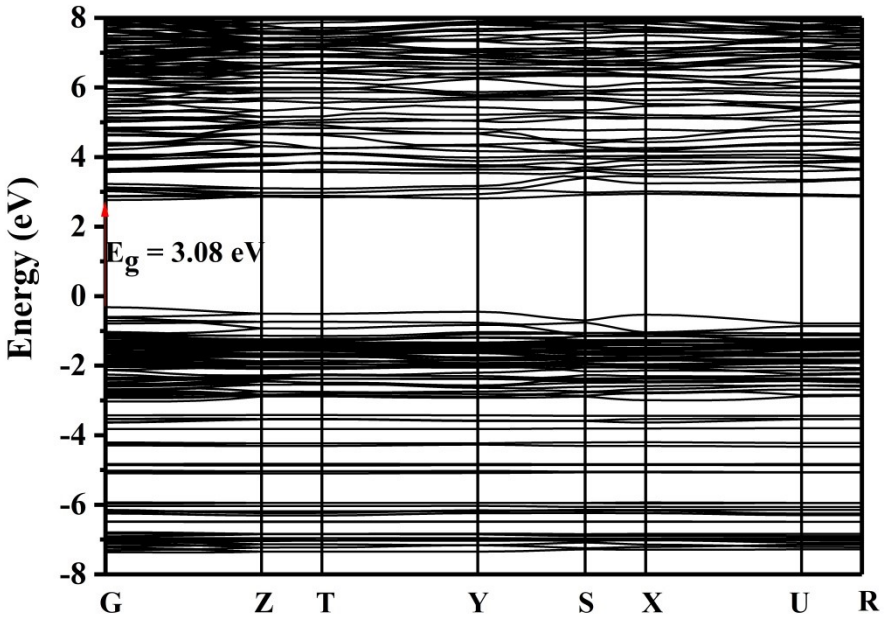

Figure S16. The calculated band structure of **$Rb_3[Pb_2Br_5(OOC(CH_2)_3COO)]$**.

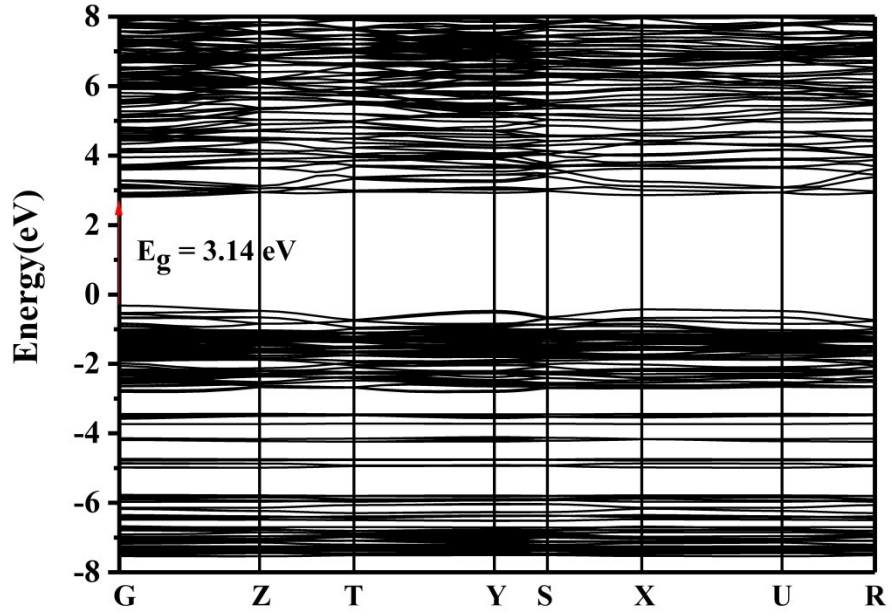

Figure S17. The calculated band structure of **$Cs_3[Pb_2Br_5(OOC(CH_2)_3COO)]$**.

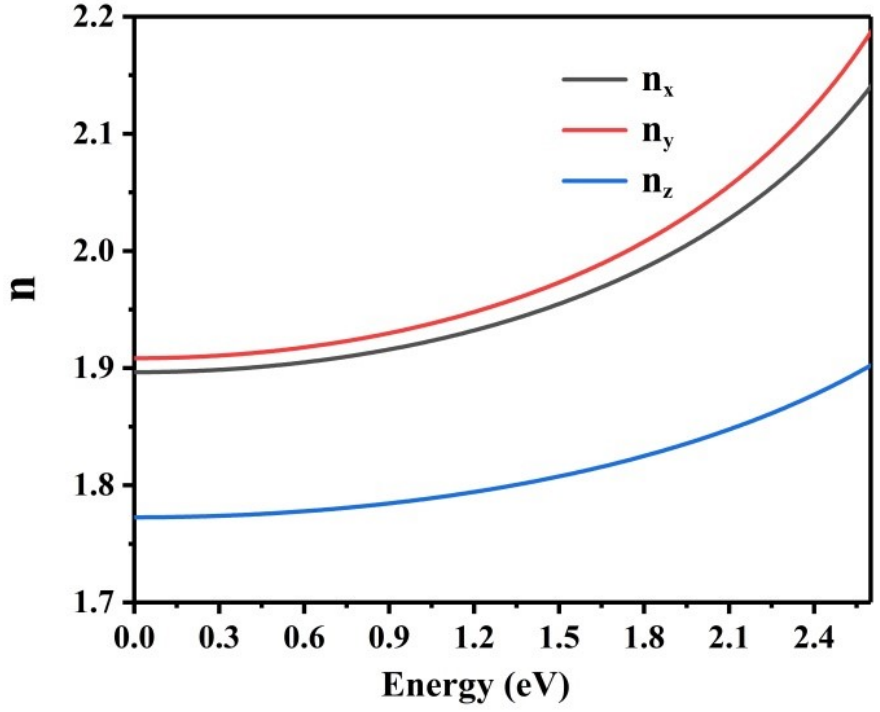

Figure S18. Optical refractive indices along principal axes *versus* photon energy for **$Cs_3[Pb_2Br_5(OOC(CH_2)_3COO)]$**.

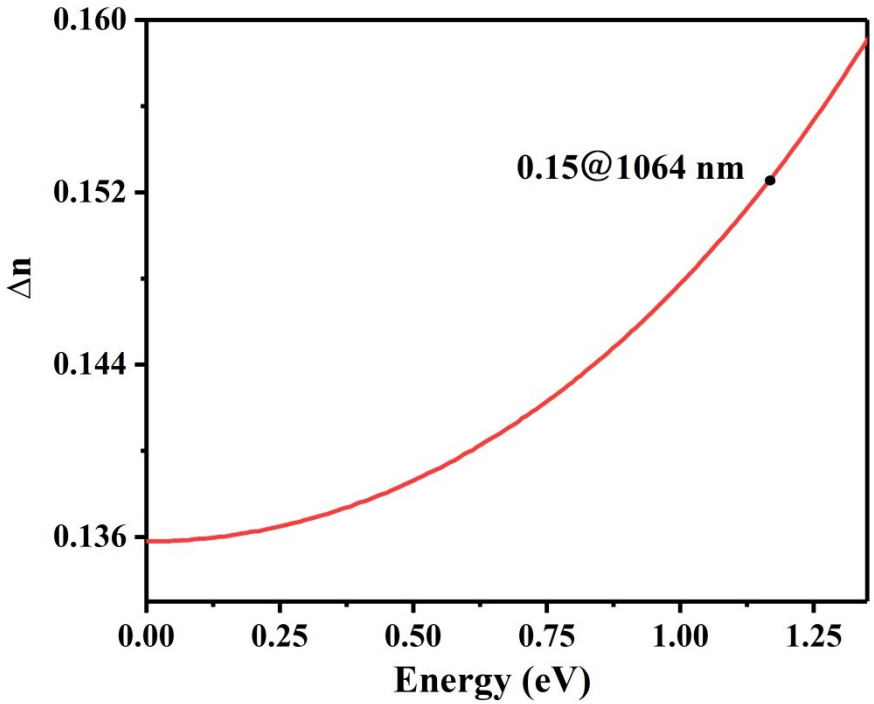

Figure S19. The calculated birefringence *versus* photon energy for **$Cs_3[Pb_2Br_5(OOC(CH_2)_3COO)]$**.

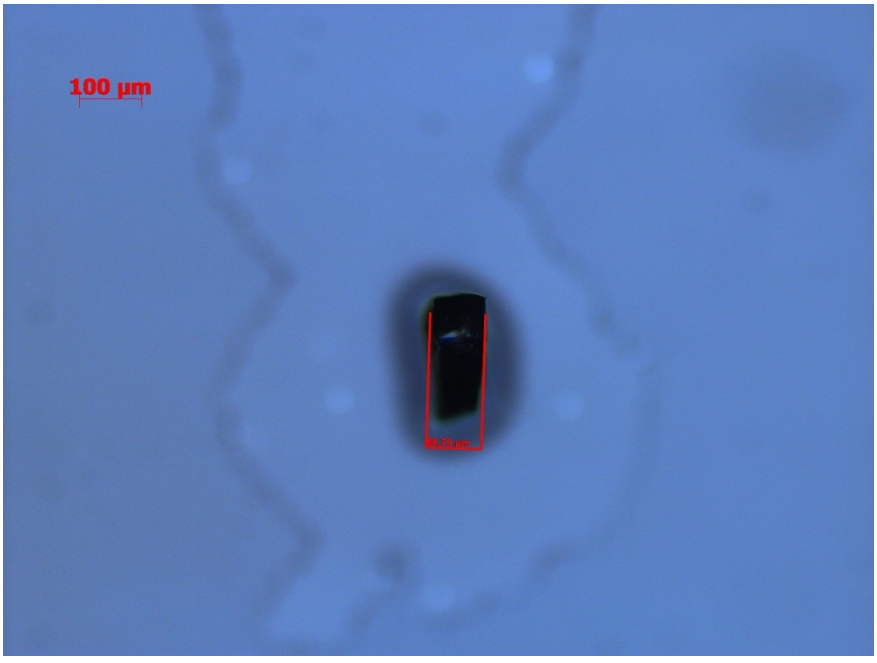

Figure S20. The original crystal for the measurement of the birefringence for **$Rb_3[Pb_2Br_5(OOC(CH_2)_3COO)]$**.

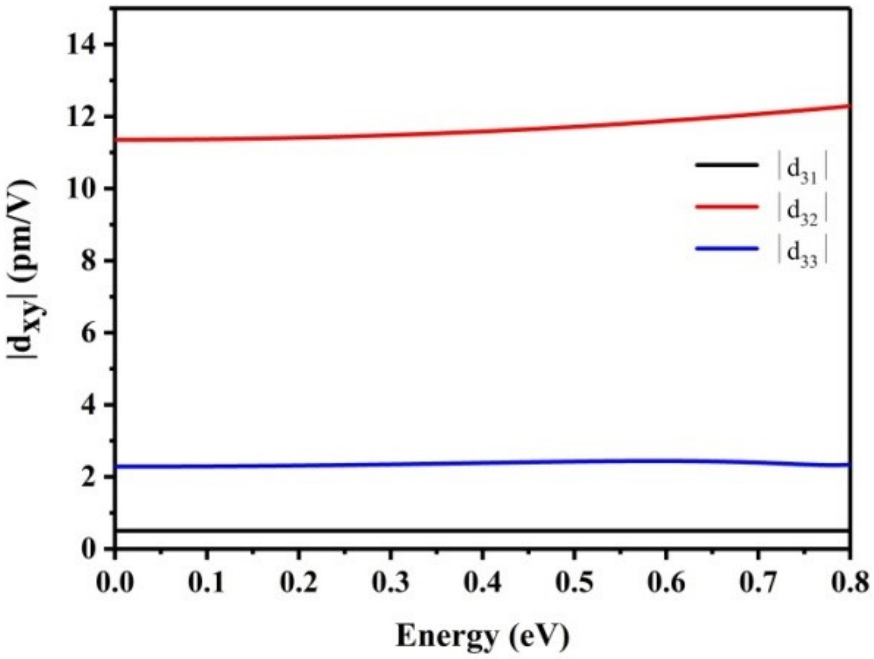

Figure S21. Frequency-dependent SHG coefficients of $|d_{31}|$, $|d_{32}|$ and $|d_{33}|$ for **$Rb_3[Pb_2Br_5(OOC(CH_2)_3COO)]$**.

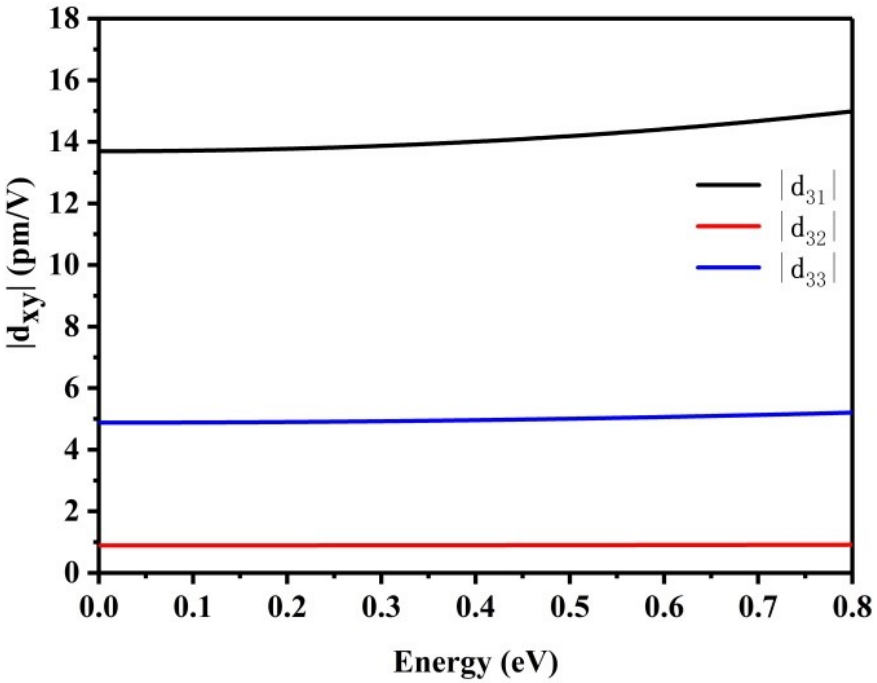

Figure S22. Frequency-dependent SHG coefficients of $|d_{31}|$, $|d_{32}|$ and $|d_{33}|$ for **$Cs_3[Pb_2Br_5(OOC(CH_2)_3COO)]$**.

References

[1] B. Champagne, D. M. Bishop, Calculations of nonlinear optical properties for the solid, Adv. Chem. Phys, 2003, 126, 41-92.

[2] A. H. Reshak, S. Auluck, I. V. Kityk, Specific features in the band structure and linear and nonlinear optical susceptibilities of $La_2CaB_{10}O_{19}$ crystals, Phys. Rev. B, 2007, 75, 245120.

[3] Y. Z. Huang, L. M. Wu, X. T. Wu, L. H. Li, L. Chen, Y. F. Zhang, $Pb_2B_5O_9I$: An iodide borate with strong second harmonic generation, J. Am. Chem. Soc, 2010, 132, 12788-12789.

[4] Y. C. Yang, X. Liu, J. Lu, L. M. Wu, L. Chen, $[Ag(NH_3)_2]_2SO_4$: A strategy for the coordination of cationic moieties to design nonlinear optical materials, Angew. Chem. Int. Ed, 2021, 60, 21216-21220.

[5] Z. Ma, J. Hu, R. Sa, Q. Li, Y. Zhang, K. Wu, Screening novel candidates for mid-IR nonlinear optical materials from I_3–V–VI_4 compounds, J. Mater. Chem. C, 2017, 1963-1972.

[6] J. P. Perdew, K. Burke, M. Ernzerhof, Generalized gradient approximation made simple, Phys. Rev. Lett, 1996, 77, 3865-3868.

[7] F. Weigend, R. Ahlrichs, Balanced basis sets of split valence, triple zeta valence and quadruple zeta valence quality for H to Rn: Design and assessment of accuracy, Phys. Chem. Chem. Phys, 2005, 7, 3297-3305.

[8] F. Weigend, Accurate coulomb-fitting basis sets for H to Rn, Phys. Chem. Chem. Phys, 2006, 8, 1057-1065.

[9] M. J. Frisch, G. W. Trucks, H. B. Schlegel, G. E. Scuseria, M. A. Robb, J. R. Cheeseman, G. Scalmani, V. Barone, G. A. Petersson, H. Nakatsuji, X. Li, M. Caricato, A. Marenich, J. Bloino, B. G. Janesko, R. Gomperts, B. Mennucci, H. P.

Hratchian, J. V. Ortiz, A. F. Izmaylov, J. L. Sonnenberg, D. Williams-Young, F. Ding, F. Lipparini, F. Egidi, J. Goings, B. Peng, A. Petrone, T. Henderson, D. Ranasinghe, V. G. Zakrzewski, J. Gao, N. Rega, G. Zheng, W. Liang, M. Hada, M. Ehara, K. Toyota, R. Fukuda, J. Hasegawa, M. Ishida, T. Nakajima, Y. Honda, O. Kitao, H. Nakai, T. Vreven, K. Throssell, J. A. Montgomery, Jr., J. E. Peralta, F. Ogliaro, M. Bearpark, J. J. Heyd, E. Brothers, K. N. Kudin, V. N. Staroverov, T. Keith, R. Kobayashi, J. Normand, K. Raghavachari, A. Rendell, J. C. Burant, S. S. Iyengar, J. Tomasi, M. Cossi, J. M. Millam, M. Klene, C. Adamo, R. Cammi, J. W. Ochterski, R. L. Martin, K. Morokuma, O. Farkas, J. B. Foresman, and D. J. Fox, Gaussian 09, Revision A.02, Gaussian, Inc., Wallingford CT, 2016.

[10] T. Lu, F. Chen, Multiwfn: A multifunctional wavefunction analyzer, J. Comput. Chem, 2012, 33, 580-592.